ELSEVIER

Thermochimica Acta 352–353 (2000) 133–139

thermochimica acta

www.elsevier.com/locate/tca

Thermal behavior of pentaerythritol diazido dinitrate

Ning Binke[a,b,*], Song Jirong[c], Hu Rongzu[b], Yu Qingsen[a], Guo Shaojun[b]

[a]*Department of Chemistry, Zhejiang University, Hangzhou 310027, PR China*
[b]*Xian Modern Chemistry Research Institute, Xian 710065, PR China*
[c]*Department of Chemical Engineering, Northwest University, Xian 710069, PR China*

Received 2 June 1999; received in revised form 30 August 1999; accepted 24 September 1999

Abstract

Under non-isothermal condition, the thermal behavior of pentaerythritol diazido dinitrate (PDADN) is studied using TG, DSC, pressure DSC and the simultaneous device of the solid reaction cell in situ/rapid scanning Fourier transform infrared (RSFT-IR) spectroscopy. The results show that (1) the extrapolated onset temperatures (T_e), peak temperatures (T_p) and enthalpy of decomposition (ΔH_{dec}) increase obviously with the change of pressure from 0.1 to 2 MPa. Over the range of pressure from 2.0 to 6 MPa, the thermal behavior of PDADN does not seem to be obviously affected by the pressure; (2) the apparent activation energy, pre-exponential constant and the most probable integral mechanism function of thermal decomposition of PDADN at the pressure of 0.1 MPa are 134.9 kJ mol^{-1}, $10^{12.7}$ s^{-1} and $1-(1-\alpha)^3$, respectively; (3) the experimental values of pressure are a principal factor affecting the magnitude of the apparent activation energy; (4) the mechanism of thermal decomposition of PDADN can be expressed by the following scheme:

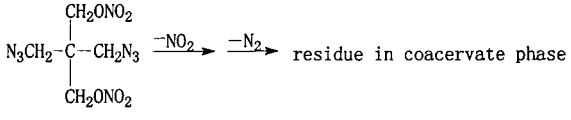

(5) the critical temperature of thermal explosive for PDADN is 423.74 K. © 2000 Elsevier Science B.V. All rights reserved.

Keywords: Kinetic parameters; Pentaerythritol diazido dinitrate; Thermal behavior

1. Introduction

Pentaerthritol diazido dinitrate (PDADN) is a novel energetic compound containing two types of energetic groups of $-ONO_2$ and $-N_3$, which can be used as an energetic azido plastizer ingredient in propellants because of its excellent performance [1–3]. Thermal behavior is one of the most important aspects of PDADN in practical application. However, its mechanism and kinetic parameters of thermal decomposition have not yet been reported. The aim of this work is to study the thermal behavior of PDADN by TG, DSC, pressure DSC and the simultaneous device of the solid reaction cell in situ/rapid scanning FT-IR (RSFT-IR) spectroscopy.

2. Experimental

2.1. Materials

PDADN was prepared in our institute. Its structure was determined by elemental analysis, IR and NMR spectroscopy. Its purity was more than 99.5%.

* Corresponding author.

0040-6031/00/$ – see front matter © 2000 Elsevier Science B.V. All rights reserved.
PII: S0040-6031(99)00457-8

2.2. Experimental apparatus and conditions

The thermal decomposition process was studied by using TG technique on a Dalta Series TGA instrument (Perkin-Elmer, USA). The conditions of TG were as follows: sample mass, about 1 mg; heating rate, 10°C min^{-1}; atmosphere, flowing nitrogen (40 ml min^{-1}, purity: 99.5%). The kinetic parameters of thermal decomposition were determined on a type of 910-DSC instrument in TA 2000 system (TA, USA). The operation conditions were as follows: sample mass, about 1 mg; heating rates, 1, 2, 5, 10 and 20°C min^{-1}, respectively; atmosphere, static nitrogen with pressures of 0.1, 2, 3 and 6 MPa, respectively. The IR spectra of PDADN and its thermal decomposition products were determined using KBr disc (4000–400 cm^{-1}) on a solid reaction cell (Xiamen University, PR China) in conjunction with 60 SXR RSFT-IR spectrophotometer (Nicolet, USA). The heating rate was 18°C min^{-1}. The sample mass was about 0.7 mg. 18 files per minute and 8 scans·per file were recorded at a resolution of 4 cm^{-1}, and IR spectra were obtained using DTGS detector.

3. Results and discussion

3.1. Thermal behavior

Typical TG and DSC curves of PDADN under the conditions described above are shown in Figs. 1 and 2. Data of thermal decomposition of PDADN obtained by DSC at various pressures are listed in Table 1.

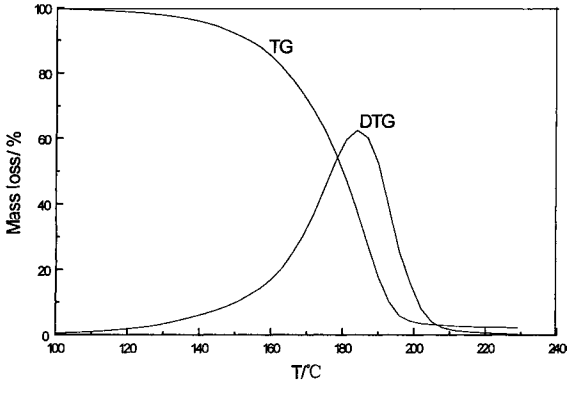

Fig. 1. Typical TG–DTG curve of PDADN at a heating rate of 10°C min^{-1}.

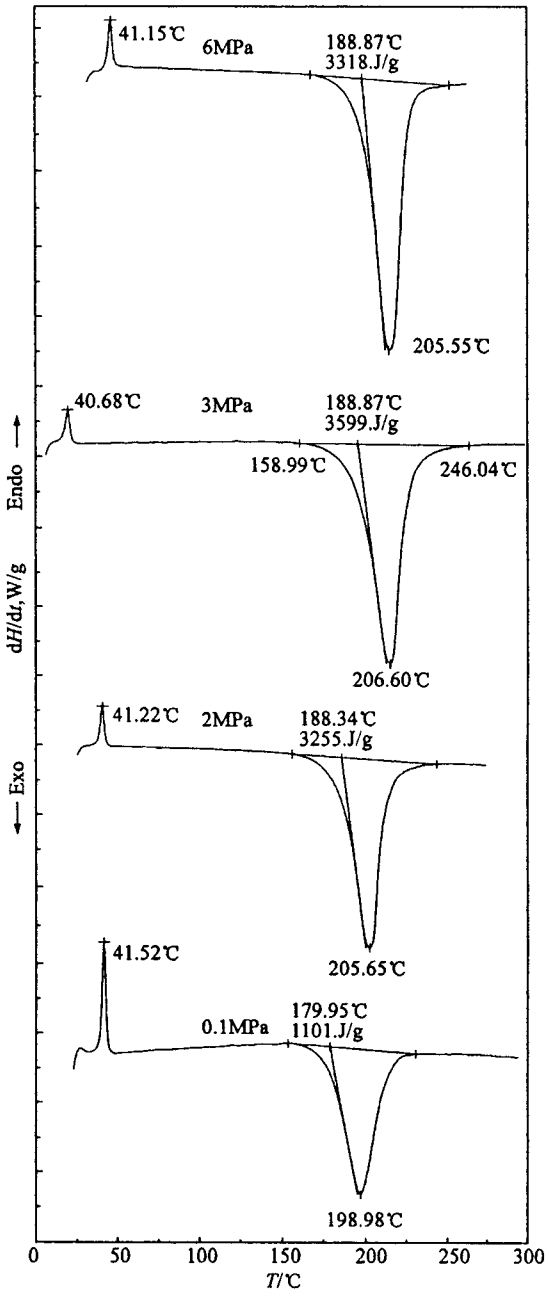

Fig. 2. Typical DSC curves of PDADN at a heating rate of 10°C min^{-1}.

It can be seen from Fig. 1 that under our conditions, the thermal decomposition process of PDADN shows only one stage on TG curve and the mass loss temperature range is from 96.38 to 248.84°C. From Fig. 2

Table 1
Data of thermal decomposition of PDADN obtained by DSC at various pressures

Pressure (MPa)	T_m (°C)	T_e (°C)	T_p (°C)	ΔH_{dec} (J g^{-1})
0.1	41.52	179.95	198.98	1101
2	41.22	188.34	205.65	3255
3	40.68	188.87	206.60	3563
6	41.15	188.87	205.55	3318

and Table 1, it is clarified that the increase of pressure is independent of the melting points of PDADN. But the extrapolated onset temperatures (T_e), peak temperatures (T_p) and enthalpy of decomposition (ΔH_{dec}) increase obviously with the change of pressure from 0.1 to 2 MPa. Over the range of pressure from 2.0 to 6 MPa, the thermal behavior of PDADN does not seem to be obviously affected by the pressure.

3.2. Kinetic equations and analysis of kinetic data

In order to obtain the kinetic parameters, the integral equation (1), Kissinger equation (2) [4] and Ozawa equation (3) [5] were used:

$$\ln\left(\frac{G(\alpha)}{T-T_0}\right) = \ln\left(\frac{A}{\beta}\right) - \frac{E}{RT} \quad (1)$$

$$\ln\frac{\beta}{T_p^2} = \ln\frac{AR}{E} - \frac{E}{RT_p} \quad (2)$$

$$\lg\beta = \lg\left(\frac{AE}{RG(\alpha)}\right) - 2.315 - 0.4567\frac{E}{RT_p} \quad (3)$$

where α is the fraction of the material reacted, $G(\alpha)$ the integral mechanism function, T_0 the initial point of the deviation from the baseline of DSC curve, β the constant heating rate, and T_p the peak temperature. E, A and R are the apparent activation energy, pre-exponential factor and gas constant, respectively.

From the DSC curves of PDADN at various pressures and heating rates, the base data in Tables 2 and 3 are obtained (where H_0 in Table 2 is total exothermicity of PDADN corresponding to the global area under the DSC curve). By substituting the base data in Table 2 and 30 types of kinetic model functions [6] into Eq. (1) by the linear least-squares method, the corresponding values of E and A and the most probable mechanism functions are obtained by the method of logical choice [6]. The results are listed in Tables 3 and 4.

Table 2
Data of PDADN determined by DSC at various pressures

Pressure (MPa)	Data point	T_i (K)	α_i
T_0=427.44 K, H_0=1156 mJ, β=10 K min^{-1}			
0.1	1	451.15	0.0362
	2	453.15	0.0500
	3	455.15	0.0681
	4	457.15	0.0914
	5	459.15	0.1214
	6	461.15	0.1592
	7	463.15	0.2056
	8	465.15	0.2613
	9	467.15	0.3260
	10	469.15	0.4007
	11	471.15	0.4840
T_0=431.72 K, H_0=3288 mJ, β=10 K min^{-1}			
2	1	459.15	0.0685
	2	461.15	0.0876
	3	463.15	0.1115
	4	465.15	0.1411
	5	467.15	0.1772
	6	469.15	0.2208
	7	471.15	0.2737
	8	473.15	0.3370
	9	475.15	0.4138
	10	477.15	0.5029
	11	479.15	0.6006
T_0=432.14 K, H_0=3527 mJ, β=10 K min^{-1}			
3	1	460.15	0.0694
	2	462.15	0.0899
	3	464.15	0.1153
	4	466.15	0.1471
	5	468.15	0.1860
	6	470.15	0.2328
	7	472.15	0.2883
	8	474.15	0.3542
	9	476.15	0.4312
	10	478.15	0.5230
	11	480.15	0.6246
T_0=431.72 K, H_0=3484 mJ, β=10 K min^{-1}			
6	1	447.15	0.0079
	2	449.15	0.0115
	3	451.15	0.0162
	4	453.15	0.0226
	5	455.15	0.0312
	6	457.15	0.0418
	7	459.15	0.0552
	8	461.15	0.0726
	9	463.15	0.0950
	10	465.15	0.1231
	11	467.15	0.1584
	12	469.15	0.2018
	13	471.15	0.2546
	14	473.15	0.3191
	15	475.15	0.3977
	16	477.15	0.4887
	17	479.15	0.5895

Table 3
The values of T_p and kinetic parameters of PDADN determined by DSC at various heating rates at the pressure of 0.1 MPa[a]

β (K min^{-1})	T_p (K)	Kissinger method			Ozawa method	
		E_k (kJ mol^{-1})	log(A/s^{-1})	r	E_0 (kJ mol^{-1})	r
1	444.76	134.47	12.88	0.9977	135.10	0.9979
2	455.17					
5	466.06					
10	474.29					
20	482.80					

[a] r is the linear correlation coefficient; E_k and E_0 are the apparent activation energy obtained by the methods of Kissinger and Ozawa, respectively.

At the constant pressure of 0.1 MPa, the values of kinetic parameters obtained by the integral method from a single non-isothermal DSC curve are in good agreement with the calculated values in Table 4 obtained by the method of Kissinger and Ozawa. Thus, the values of E of 134.9 kJ mol^{-1} and A of $10^{12.7}$ s^{-1} are believed to be for the thermal decomposition of PDADN at the pressure of 0.1 MPa.

The kinetic parameters and the most probable mechanism functions of the thermal decomposition of PDADN under the conditions of other pressures obtained by the integral method are summarized in Table 4. It can be seen from Table 4 that the form of the most probable mechanism function is similar to that of the most probable mechanism function at the pressure of 0.1 MPa. With increasing pressure, the values of E increase, indicating that the increase of pressure leads to inhibition of the thermal decomposition reaction.

3.3. Thermal decomposition mechanism

The typical IR spectra of the condensed phase products at different temperatures during the thermal decomposition process of PDADN are shown in Fig. 3. The corresponding two-dimensional curves for the FT-IR relative absorbance intensity vs. time and temperature are shown in Fig. 4.

It can be seen from Figs. 3 and 4 that with increase of temperature, the intensity of the NO_2 band at 1643 and 1281 cm^{-1} decreases gradually first until disappearance at 201.4°C, and that of N_3 group at 2112 cm^{-1} decreases later until disappearance at 239.6°C. This fact shows that the nitro group is first cleaved from PDADN, and then the N_3 group is cleaved. With increase of temperature, a new weak band appears at 1380 cm^{-1}, which may be assigned to nitrate ions formed according to Eq. (4). Its intensity increases gradually with increase of temperature, which shows that the decomposition product containing nitrate ions is formed.

$$2NO_2 + KBr = KNO_3 + NOBr \quad (4)$$

The characteristic absorption band of CN group appearing at 2244 cm^{-1} is caused by the denitrogeneration during the thermal decomposition of PDADN. With increase of temperature, its intensity increases up to the maximum at 210.8°C indicating that the product containing CN group is present in residue in coacervate phase. On the basis of above-mentioned experimental result, the thermal decomposition mechanism

Table 4
Results of the thermal decomposition of PDADN at various pressures (β=10°C min^{-1})

Pressure (MPa)	$G(\alpha)$	E (kJ mol^{-1})	log(A/s^{-1})	r	s[a]
0.1	$1-(1-\alpha)^3$	134.99	12.54	0.9891	0.02533
2	$1-(1-\alpha)^{1/2}$	165.34	15.13	0.9999	0.00242
3	$1-(1-\alpha)^{1/2}$	169.75	15.59	0.9999	0.00106
6	$1-(1-\alpha)^{1/2}$	186.63	17.45	0.9998	0.07394

[a] Standard deviation.

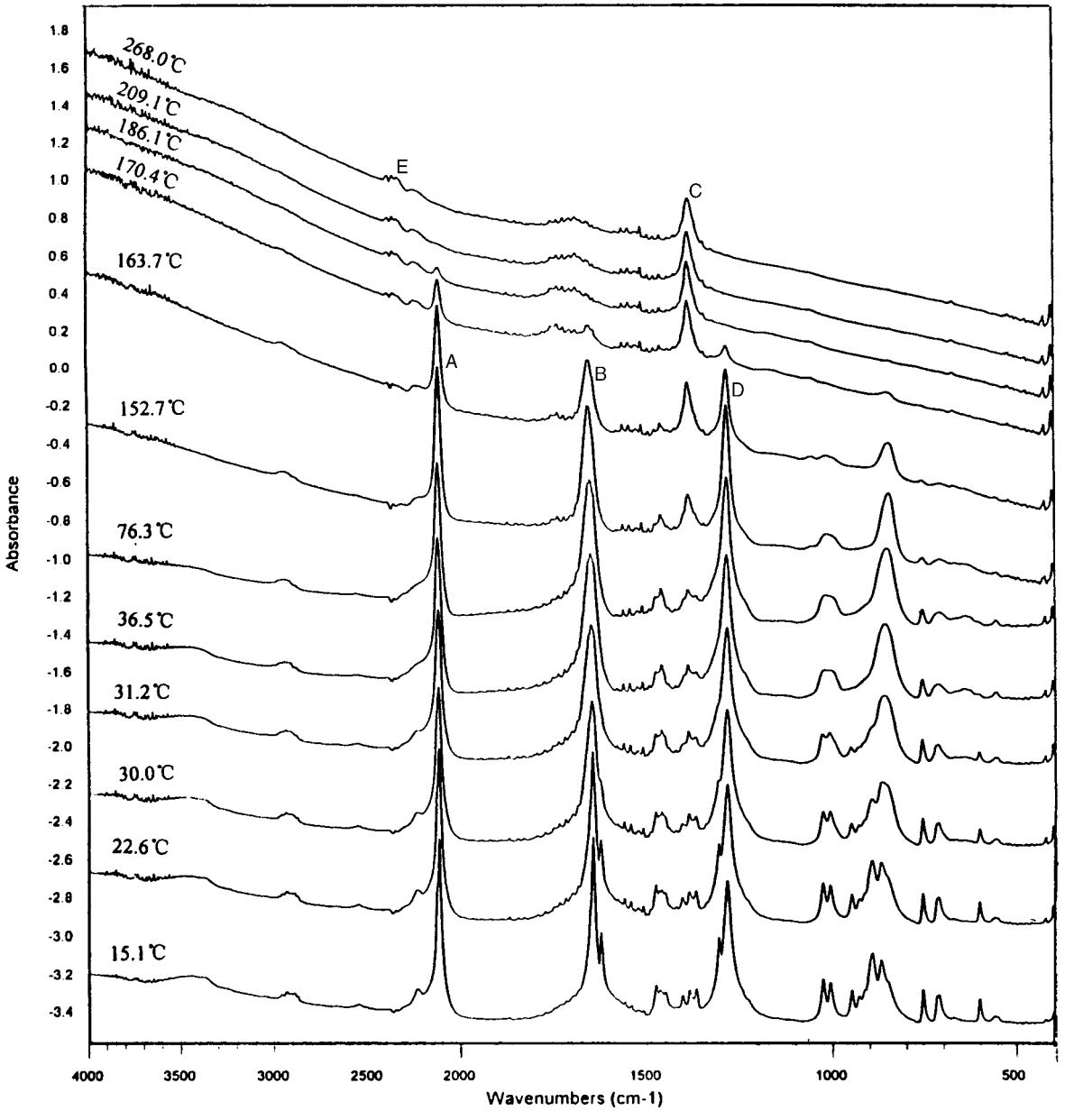

Fig. 3. The typical IR spectra of PDADN and its condensed phase products at different temperatures during the thermal decomposition process of PDADN (A: N_3, 2112 cm^{-1}; B: NO_2, 1643 cm^{-1}; C: NO_3^{-1}, 1380 cm^{-1}; D: NO_2, 1281 cm^{-1} ; E: CN, 2244 cm^{-1}).

of PDADN is postulated to be as follows:

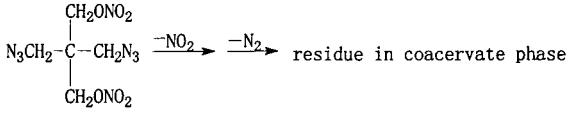

3.4. Critical temperature of thermal explosive

In order to obtain the critical temperature of thermal explosive (T_b) for PDADN, Eq. (5) in [7] was used.

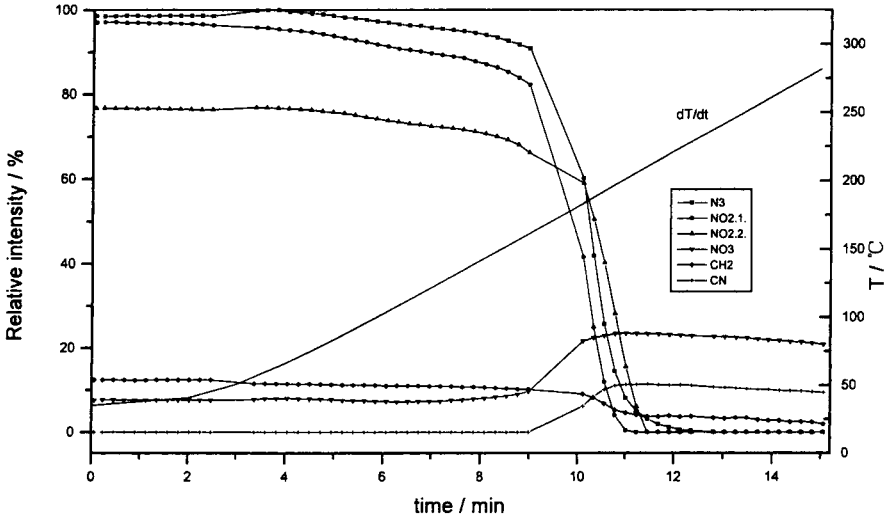

Fig. 4. The two-dimensional curves for the relative intensity of the characteristic groups of PDADN and its thermal decomposition products vs. time and temperature (A: N_3, 2112 cm^{-1}; C: $NO_3{}^{-1}$, 1380 cm^{-1}; D: NO_2, 1281 cm^{-1}; E: CN, 2244 cm^{-1}; F: CH_2, 868 cm^{-1}).

Table 5
The initial data determined by DSC and the calculated result of T_b

β/K min^{-1}	T_e/K	E_{ke}/kJmol^{-1}	T_{e0}/K	T_b/K
20	457.77	132.56		423.74
10	451.65			
5	441.41			
2	434.20			
1	423.25			
$\beta\rightarrow 0$			412.48	

$$\frac{E_{ke}}{RT_b^2}(T_b - T_{eo}) = 1 \quad (5)$$

where E_{ke} is the apparent activation energy obtained by Kissinger method with treatment of β_i and T_{ei}, T_{eo} is the extrapolated onset temperature corresponding to $\beta\rightarrow 0$. Substituting the values of E_{ke} and T_{eo} listed in Table 5 into Eq. (5), the value of T_b of 423.74 K for PDADN is obtained.

4. Conclusions

1. The extrapolated onset temperatures (T_e), peak temperatures (T_p) and enthalpy of decomposition (ΔH_{dec}) increase obviously with the change of pressure from 0.1 to 2 MPa. Over the range of pressure from 2.0 to 6 MPa, the thermal behavior of PDADN does not seem to be obviously affected by the pressure.
2. The apparent activation energy, pre-exponential constant and the most probable integral mechanism function of thermal decomposition of PDADN at the pressure of 0.1 MPa are 134.9 kJ mol^{-1}, $10^{12.7}$ s^{-1} and $1-(1-\alpha)^3$, respectively.
3. The experimental values of pressure are the principal factor affecting the magnitude of the apparent activation energy.
4. The mechanism of thermal decomposition of PDADN can be expressed by the following scheme:

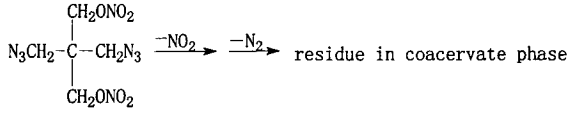

5. The critical temperature of thermal explosive for PDADN is 423.74 K.

References

[1] M.B. Frankel, E.R. Wilson, USP 4 683 086, 1987.

[2] Wang Xiaochuan, Li Shunxiu, Huang Yue, Li Changqing, Energ. Mater. 2 (3) (1994) 29–35 (in Chinese).
[3] Guo Shaojun, Su Songqin, Zahng Lijie, He Ying, Proceedings of the Third Beijing International Symposium on Pyrotech. and Explos., BIT press, Beijing, 1995, pp. 143–145.
[4] H.E. Kissinger, Anal. Chem. 29 (1957) 1702.
[5] T. Ozawa, Bull. Chem. Soc. Jpn. 38 (1965) 1881.
[6] Hu Rongzu, Yang Zhengquan, Liang Yanjun, Thermochim. Acta 123 (1988) 135.
[7] Zhang Tonglai, Hu Rongzu, Xie Yi, Li Fuping, Thermochim. Acta 244 (1994) 171.